International Journal of Mathematical, Engineering and Management Sciences
Vol. 7, No. 2, 258-271, 2022
https://doi.org/10.33889/IJMEMS.2022.7.2.017

A Comparative Study of Gradient Descent Method and a Novel Non-Gradient Method for Structural Shape Optimization

Ishan Jha
Department of Civil Engineering,
Indian Institute of Technology - BHU, Varanasi, Uttar Pradesh, India.
Corresponding author: ishan.jha.rs.civ18@iitbhu.ac.in

Krishna K. Pathak
Department of Civil Engineering,
Indian Institute of Technology - BHU, Varanasi, Uttar Pradesh, India.
E-mail: kkpathak.civ@iitbhu.ac.in

Mrigank Jha
Department of Mechanical Engineering,
Indian Institute of Technology - Jammu, J&K, India.
E-mail: 2020pth0052@iitjammu.ac.in

Ashutosh Ranjan
Department of Mechanical Engineering,
Birla Institute of Technology - Mesra, Ranchi, India.
E-mail: mtmec10009.20@bitmesra.ac.in

(Received on August 7, 2021; Accepted on January 31, 2022)

Abstract
Motivated by the works on non-gradient techniques in the domain of shape optimization of the structure, the present work intends to suggest a novel non-gradient procedure for shape optimization of structures and compare it to an existing gradient-based method. The presented technique optimizes the shape of structural parts using a fuzzy controlled integrated zero-order methodology incorporating the notion of design elements and automated mesh construction with mesh refinement at each iteration. The movement of nodes and convergence monitoring is taken care of using the triangular fuzzy membership function. The changes in shape occur according to the selected target maximum shear stress (σ_t) with a view of reaching as near to the target as possible at all the points. The present methodology is packaged in a piece of software termed GSO (Gradientless shape optimization) coded in FORTRAN language. To explain the efficacy of the current approach, a few basic structural shapes have been optimized under various constraints, and the results of the same are compared to those obtained using Optistruct (a part of software suite HyperWorks from Altair engineering), which works on gradient descent method. The proposed approach works well and produces more industry fabricable results than what is produced by the gradient descent method in Optistruct.

Keywords- Shape optimization, Fuzzy set, Fuzzy membership function, Finite element, Non-gradient, Design element, Optistruct.

1. Introduction

In the era of wanting to have the best returns for the best possible cost minimization, it is very necessary even in the engineering field to have minimised cost of construction without compromising with the strength and serviceability of the structures. Optimized structures are becoming part of our lives as the adoption rate of such structures has increased significantly. Along the time, many different ways (Mei & Wang, 2021) to optimize the structure have come

up, viz. topology optimization, size optimization, topography optimization, shape optimization etc. All the different ways of optimization have proved their utility in the real world, among which shape optimization techniques have been gaining popularity over time (Upadhyay et al., 2021) as it enhances the structure's fundamental shape without adding additional cut-outs or holes while adhering to the parameters laid over it. Shape optimization found its root in 1638 when Galileo first tried to optimize a cantilever beam as a parabolic profile. Many research works for getting the optimized shape of structure using various algorithms have been successfully worked upon (Munk et al., 2015) since then. However, almost all the shape optimization algorithms can broadly be classified in two genres (Pathak et al., 2007): (1) Non-gradient/ zero-order method, (2) Gradient-based method. Out of these, Gradient-based methods has much more widely been accepted around the globe, and almost all the optimization software works on gradient-based method while cornering out the non-gradient methods and works done on it. Due to this, the studies on non-gradient methods in shape optimization of structures have often been neglected despite proving its efficiency and practicality over gradient-based methods.

Initial works on non-gradient methods can be seen (Mattheck, 1989; Mattheck & Burkhardt, 1990; Baumgartner et al., 1992; Chen & Tsai, 1993) using ideas motivated from living things where they recommended material addition at the higher stressed area and material removal from lower stressed areas to achieve an optimal shape of the structure. Many different methods, such as Simulated Annealing and its effects on the final design (Shim & Manoochehri, 1997; Dong et al., 2020), Immune Algorithms inspired by biological immune systems (Luh & Chueh, 2004), Harmony Search explicated the basis of the musical process to find the perfect harmony state (Lee & Geem, 2004), Genetic Algorithms (Wang & Tai, 2005; Guest & Genut, 2010; Manan et al., 2010; Balamurugan et al., 2008, 2011), Ant Colonies optimization inspired from ants behaviour to reach its food via shortest path (Kaveh et al., 2008), Particle Swarm optimization techniques (Luh et al., 2011), Bacterial Foraging algorithms which is another bio-inspired technique (Georgiou et al., 2014) and many others have been devised as non-gradient approaches in the domain of optimization. However, not many techniques have been used for shape optimization. One of the most famous non-gradient shape optimization algorithms was Evolutionary Structural Optimization (ESO) technique. Early use of (ESO) was done by Rispler et al. (2000) for designing adhesive fillets.

Bennett and Botkin (1985) developed a geometric problem description format that used only boundary information. They also incorporated the adaptive mesh refinement scheme to get more accurate solutions. Berke et al. (1992) applied artificial neural networks to get the optimized design for structural components used in aerospace. Hasengawa (1992) gave two methods based on zero-order technique, one for the change of thickness and another for the change of coordinates on the boundary. Wu (2005) took the reduction of stress concentration factor under consideration for optimization of the shape of structures using the zero-order method. Jarraya et al. (2007) considered the linear behaviour of the beam for shape and thickness optimization. They used the sequential quadratic programming (SQP) method. Nagy et al. (2009) developed an analytical isometric technique for optimizing the beam's shape by varying the position of control points and structural weight. Mortazavi (2020a, 2020b) proposed a metaheuristic technique based on fuzzy algorithms for parameter-free optimization of large scale structures. These studies have proved the effectiveness of non-gradient methods in the field of shape optimization.

Continuing and taking inspiration from previous works, the present study presents a novel integrated zero-order method using fuzzy membership functions. The current approach incorporates automated mesh construction and its refinement occurring at every single completed iteration with the concept of design elements to achieve a streamlined silhouette and eliminate unwanted jagged edges. The previous methods used so far in industries are unable to remove sharp corners and jagged edges, causing too many regions of stress concentration. These have been addressed and taken care of in this approach. The mobility of design nodes as well as the ultimate convergence are controlled using fuzzy set theory. This proposed approach is based upon the notion of non-gradient shape optimization and packaged in a piece of software termed GSO (Gradientless shape optimization) coded in FORTRAN language. The current approach attempts to establish the efficiency of non-gradient methods and prove their competence in the field of shape optimization. To have a basic understanding of the effectiveness of the current approach, a few basic structural shapes have been optimized, and results of which are compared to the results obtained by a gradient descent method used by Optistruct, which is a part of software suite HyperWorks from Altair engineering.

Optistruct is one of the heavily used software for structural shape optimization by industries and researchers. It works on the Gradient descent method, also sometimes called Gradient Method. It uses the gradient value to find the minimum of the function. The local approximation method assuming small changes in the design at each optimization step is used. Solution of approximate optimization problems based on sensitivity data is used for design updates. Optistruct is equipped with three different methods viz; primal feasible direction method, a dual method and optimality criteria method. The shape optimization in optistruct uses the primal feasible direction method, which is based on convex linearization of design space. At the same time, the others are used in other forms of optimization. The proposed approach (GSO) seems to give a more industry-friendly and fabricable final optimized shape of structure compared to the Optistruct.

1.1 Optimization Procedure: GSO

The present work proposes an integrated zero-order method for model generation and its shape optimization. The approach targets the effectiveness of shape optimization and its adaptability to various complexities. It is developed to provide a nifty geometric depiction of the model's boundaries. The generated finite element model changes shape at each iteration, causing possible distortion of elements. To take care of this updated finite element mesh is generated at each iteration using iso-parametric mapping technique (Zienkiewicz & Taylor, 1991; Krishnamoorthy, 1994) and the conception of design elements, ensuring the use of a single design variable for governing both meshing and optimization. The optimised model is first fragmented into the desired set of design elements; each defined using eight keynodes, also called master nodes that regulate the shape of design elements. These master nodes then additionally subdivide the design elements into finite elements. Figure 1 depicts a possible discretization of the beam with the location of master nodes.

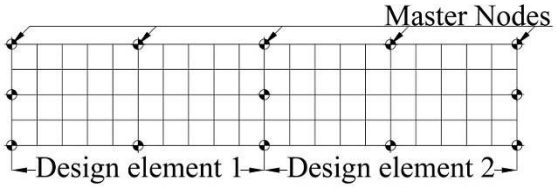

Figure 1. Representation of probable design elements and location of master nodes.

The boundary key nodes being evaluated for optimization are considered as design nodes. They bear specific coordinates, which is taken up as design variables. Coordinates of the newly obtained nodes are derived using iso-parametric mapping. Considering *'X'* and *'Y'* as coordinates of the obtained node, it is represented by Eq. (1):

$$X = \sum_{i=1}^{N_m} N_i(\xi,\eta) \cdot X_i$$
$$Y = \sum_{i=1}^{N_m} N_i(\xi,\eta) \cdot Y_i \quad (1)$$

Where, *'i'* is the considered master/key node with X_i and Y_i as its co-ordinates, (ξ, η) represents the natural co-ordinates of (X, Y), N_m and N_i indicate the total count of mater/key node and shape function respectively. The optimizer passes the changed coordinates for each master/key node onto the mesh constructor for the construction of fresh mesh at each iteration. For the finite element modelling, nine noded Lagrangian elements are used in the current study.

1.1.1 Fuzzy Membership Function

The use of fuzzy techniques in shape optimization has been done for a long time (Mohandas et al., 1990; Soh & Yang, 1996). New fuzzy strategies in the field of optimization have come up from time to time. Recently, Mortazavi (2020a, 2020b) proposed a new fuzzy approach that reduced the complexity of topology and size optimization in structures through transforming complicated search spaces in fuzzy domains. Cuevas et al. (2020) published a chapter on optimization based on fuzzy logic proposing a methodology to imitate the human experience of searching in an algorithm. We, in our approach, have used the idea of a fuzzy membership function (Zimmermann, 1996; Chaube & Singh, 2016; Kumar et al., 2021). A target maximum shear stress (σ_t) is defined beforehand, and at each iteration, the shape changes so as to achieve maximum shear stress (σ) at key/design nodes as close as possible to the defined σ_t. For the present work, the triangular shape membership (Kosheleva et al., 2018) function is utilized to determine the shape whose σ value is closest to σ_t. The membership value (μ) and σ_t exhibit a linear correlation between them because of the triangular membership function. When at the design nodes σ is equal to σ_t, μ becomes equal to 1, as shown in Figure 2. Eq. (2) expresses the relation analytically.

$$\mu(\sigma) = \begin{Bmatrix} \frac{\sigma}{\sigma_t} & if \sigma < \sigma_t \\ 1 & if\ \sigma = \sigma_t \\ 2 - \frac{\sigma}{\sigma_t} & if\ \sigma_t < \sigma < 2\sigma_t \\ 0 & if\ \sigma > 2\sigma_t \end{Bmatrix} \quad (2)$$

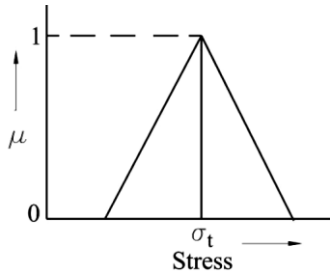

Figure 2. Triangular function.

The addition of material is done when σ is greater than σ_t, and subtraction contrariwise at each iteration till both the σ and σ_t becomes more or less equal. The current work permits a deviation of ≤ 1 N/mm^2 of stress value between σ and σ_t. The change in coordinates for the considered i^{th} node is presumed in proportion to the move factor (MF), which is related to σ_i and σ_t as expressed by Eq. (3). The plot of MF versus σ_t is shown in Figure 3:

$$MF = \begin{Bmatrix} \mu\,(\sigma_i) - 1 & if \sigma_i > \sigma_t \\ 1 - \mu(\sigma_i) & if \sigma_i < \sigma_t \end{Bmatrix} \quad (3)$$

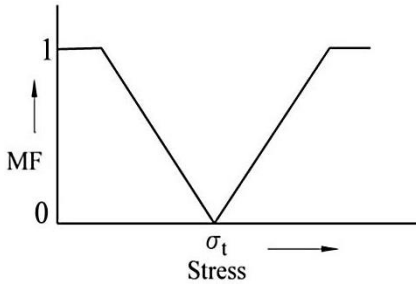

Figure 3. Move factor.

The motion of the design nodes is depicted in Figure 4. The middle node '*j*' is chosen as the direction node, and the design node, represented by node '*i*', move-in compliance to node '*j*'. The smallest length among all the lengths between the design node and its corresponding direction node is symbolized by L_{min} defined analytically by Eq. (4):

$$L_{min} = \min_{i=1}^{N_d} (L_i) \quad (4)$$

Where, $L_i = \sqrt{(X_i - X_j)^2 + (Y_i - Y_j)^2}$ and N_d represents total design nodes.

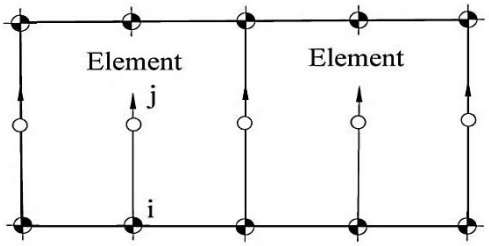

Figure 4. Direction node.

The nodal movement of nodes in the study has been allowed for the entire L_{min} and is expressed by Eq. (5):

$$MV\,(i) = 1.0 \cdot L_{min} \cdot MF \quad (5)$$

At each iteration, the modification of coordinates for the considered design node '*i*' is expressed using Eq. (6):

$$X_i' = X_i + (X_j - X_i) \cdot \frac{MV(i)}{L_i}$$
$$Y_i' = Y_i + (Y_j - Y_i) \cdot \frac{MV(i)}{L_i} \quad (6)$$

Where, X_i' And Y_i' are the freshly accquired co-ordinate and (X_i, Y_i) and (X_j, Y_j) are the direction node coordinates. As the fresh co-ordinate value is procured, the information is taken by the optimizer and conveyed onto the mesh constructor for the construction of fresh mesh for subsequent stress analyzation. This step is continued repeatedly unless the convergence criterion is achieved.

1.2 Optimization Procedure: Optistruct

To account for the structural shape change and its reflection on interior mesh in order to avoid mesh distortion, Optistruct uses a perturbation vector approach. The change in the shape of the structure is based on the linear combination of perturbation vectors. Approximate probable shapes are at first defined as perturbations added to the vector of nodal coordinates (X_0, Y_0), as shown in Figure5. Using a linear combination of the perturbations vectors, a change in structural shape is achieved. The final mesh nodal movement is given by Eq. (7)

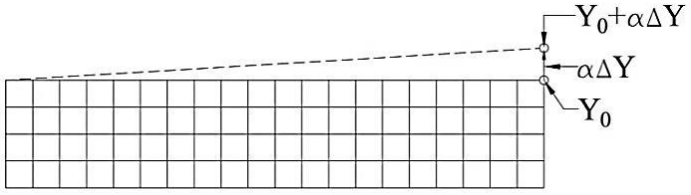

Figure 5. Description of shape design variable.

$$\left.\begin{aligned} X &= X_0 + \sum_{i=1}^{n} \beta_i \Delta X_i \\ Y &= Y_0 + \sum_{i=1}^{n} \alpha_i \Delta Y_i \end{aligned}\right\} \quad (7)$$

Where X, Y is the vector of nodal co-ordinates for the changed shape, X_0, Y_0 is the vector of nodal co-ordinate for initial shape, n is the number of shape/ design variables, β and α are the magnitudes of perturbation, ΔX and ΔY are the perturbation vector. For the present study, weight is minimized under the constraint of maximum shear stress.

1.3 Convergence Criteria: GSO

Due to the fuzziness of the stress pattern, it is tough to satisfy the optimum conditions of membership function value which is equal to 1. To address this, fuzzy interaction generally identified as minimum membership function (MMF) is implemented. The change in the value of MMF at each iteration is indicative of convergence. As the value reaches the maximum and then starts to decline for three successive iterations, the programme is terminated, and the criterion for convergence is declared to be satisfied. It can mathematically be composed of as Eq. (8):

$$\mu(\sigma_{iteration}) = \min_{i=1}^{N_d} (\cap \mu\,(\sigma_i)) \quad (8)$$

If, $\mu\,(\sigma_{iteration}) < \mu\,(\sigma_{iteration} + 1)$ proceed for next iteration.
If, $\mu\,(\sigma_{iteration}) > \mu\,(\sigma_{iteration} + 1)$ iteration stops and convergence criterion is achieved.

1.4 Convergence Criteria: Optistruct

Optistruct uses two types of convergence criteria, viz. regular convergence and soft convergence. When for two consecutive iterations the constraint violation remains below 1%, and change in the value of objective function remains less than objective tolerance, the regular convergence is said to be achieved. Since the convergence is based on a comparison of the latest objective values, a minimum of three analyses is needed for regular convergence. On the other hand, soft convergence is said to be attained if the design variable shows hardly any variation for two successive iterations. Regular convergence takes one iteration more than soft convergence.
The working steps of GSO and Optistruct are shown as flowcharts in Figure 6.

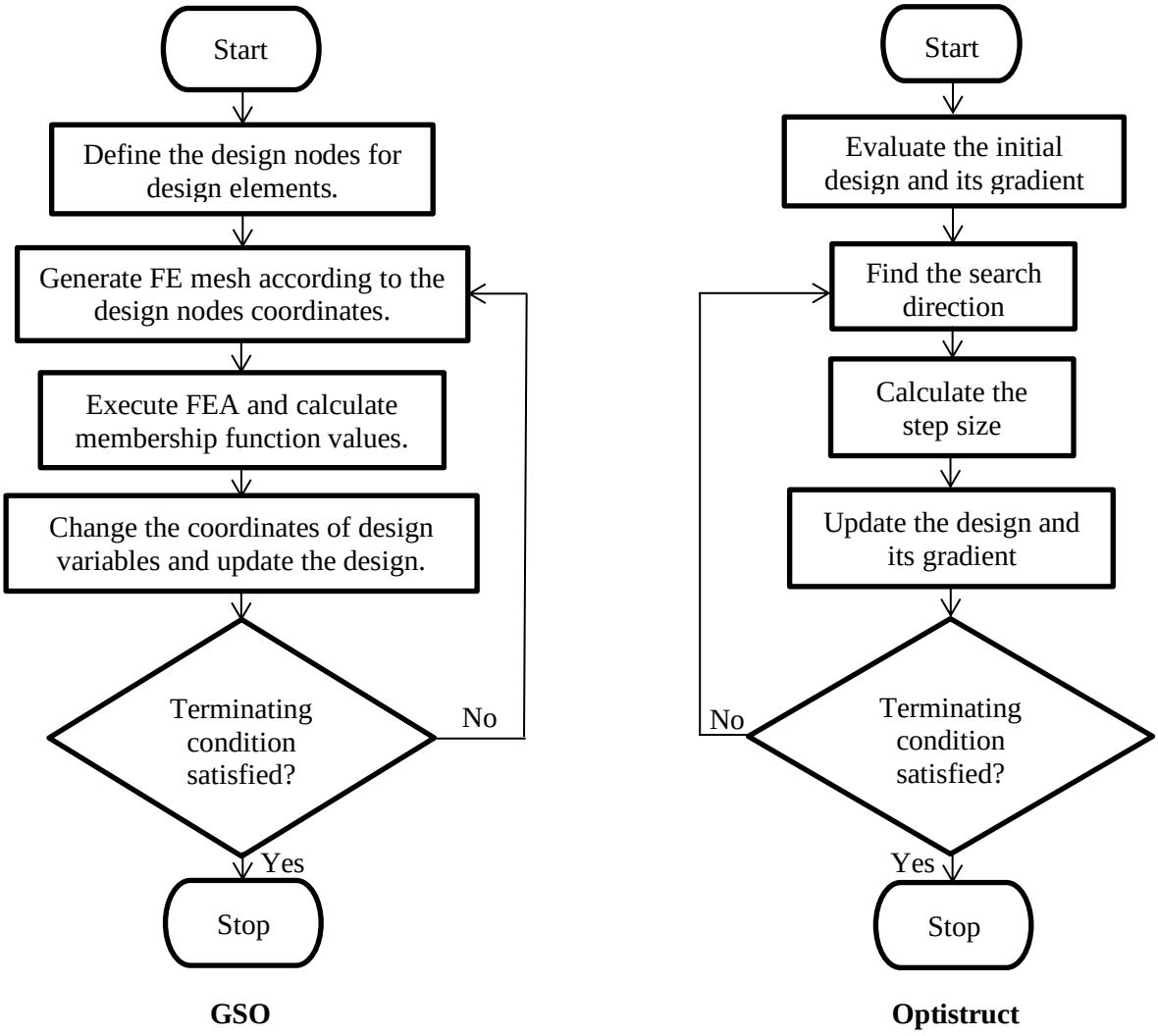

Figure 6. Flowchart for working steps in GSO and Optistruct.

2. Mesh Convergence and Validation Study

For the mesh convergence and validation study, a fixed beam having linear-elastic properties ($E=2.1x10^5$ N/mm^2 , ν =0.3 and ρ = 7.85 $x10^{-5}$ N/mm^3), dimensions as (1000x150x100) mm with point load of 100 kN at the centre is taken. The model is prepared in both Hypermesh and GSO with varying average element size from 200 to 5 and is compared with the bending stress (Φ) calculated using the conventional formula (Formula A) $\Phi = M/Z$. The result of the study is presented in Figure 7. It is noticed that the hypermesh model converges at an average element size of 10, whereas the GSO model gets converged early at a relatively bigger average element size of 50. The average element size of 10 and 50 is now used successively hereafter for present analysis in Optistruct and GSO, respectively.

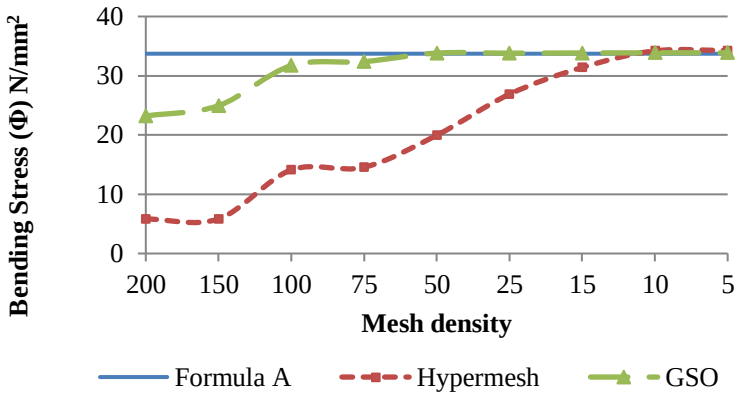

Figure 7. Mesh convergence and validation

3. Numerical Illustrations and Discussion

After validation and mesh convergence study, a few problems with different optimization parameters have been worked out to compare the optimized shape under the two different approaches. The target maximum shear stress is tried to be achieved while reducing the overall weight for the final optimized shape. Three different types of beams (B1, B2 and B3) and one circular plate with a square cut-out (CC) is considered for the present study. The structures are also checked for permissible deflection criteria according to the IS 456:2000, so that the obtained final optimized shape doesn't end up failing the serviceability criteria. The first beam (B1) is a straight beam simply supported on its edges with a concentrated point load at its centre. The B1 beam is optimized under a design constraint of keeping the top flat. For this, in GSO design, nodes on the bottom face of the beam have only been allowed to move, and in Optistruct design, variables on the bottom face have only been given. The second beam (B2) is a curved beam fixed on its ends with two concentrated point loads placed asymmetrically, as indicated in Table 2. The B2 beam is optimized from both top and bottom and compares the effect of asymmetric loading on optimized shape obtained by the two different methods. The circular plate (CC) is loaded with a uniformly distributed load along its circumference. As a result of the symmetry of the circular plate, only a quarter part is being considered and analysed for shape optimization. The shape of the cut-out is optimized and compared in this illustration. For the further studies if not mentioned, the material properties are taken as ($E = 2.1x10^5$ N/mm^2, $\nu = 0.3$ and $\rho = 7.85\ x10^{-5}$ N/mm^3). The number of iterations and the system time taken by GSO and Optistruct to get the optimized shape of B1, B2 and CC and the percentage weight reduction and final optimized shape are shown in Table 1, Table 2 and Table 3, respectively.

Table 1. Parameters for B1 with iterations, runtime and percentage weight reduction to reach the optimized shape.

Type of structure	Dimensions (mm)	Loading	σ_t (N/mm^2)	Iterations (Nos.)		Runtime (Sec.)		Weight Reduction (%)		Max. deflection (mm)	
				GSO	Optistruct	GSO	Optistruct	GSO	Optistruct	GSO	Optistruct
B1 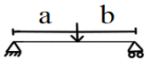	L = 1000 H = 150 D = 50 a = b =500	Point Load (60 kN)	40	28	5	07	10	25.58	15.74	0.937	0.839
		Final optimized shape									
		GSO 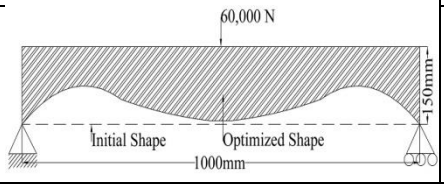						Optistruct 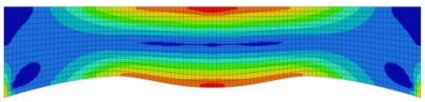			

Table 2. Parameters for B2 with iterations, runtime and percentage weight reduction to reach the optimized shape.

Type of structure	Dimensions (mm)	Loading	σ_t (N/mm^2)	Iterations (Nos.)		Runtime (Sec.)		Weight Reduction (%)		Max. deflection (mm)	
				GSO	Optistruct	GSO	Optistruct	GSO	Optistruct	GSO	Optistruct
B2 	Cur. L = 800 H = 100 D = 100 a = 300 b = 150	Two point load (40 kN and 40 kN)	20	177	5	22	09	20.18	41.27	0.084	0.116
		Final optimized shape									
		GSO 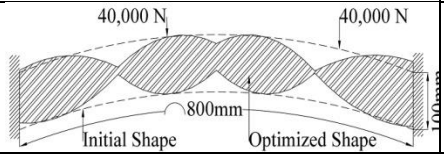						Optistruct 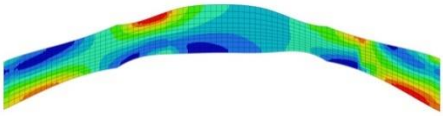			

Table 3. Parameters for CC with iterations, runtime and percentage weight reduction to reach the optimized shape.

Type of structure	Dimensions (mm)	Loading	σ_t (N/mm^2)	Iterations (Nos.)		Runtime (Sec.)		Weight Reduction (%)	
				GSO	Optistruct	GSO	Optistruct	GSO	Optistruct
CC 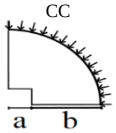	R = 600 D = 5 a = 100 b = 500	Uniformly distributed load (0.1 kN/mm)	20	69	4	09	10	15.04	18.69
		Final optimized shape							
		GSO 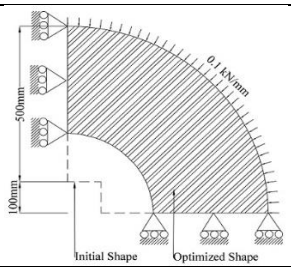					Optistruct 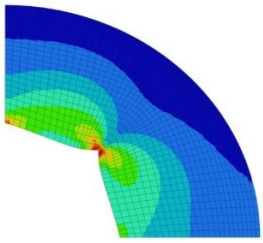		

The third beam (B3) is a composite beam made up of two different materials fixed at the ends with a uniformly distributed load throughout. Beam B3 compares the effect of change of material properties on the optimized shape obtained. For this, the beam B3 is further made into five different types of beams (B3a, B3b, B3c, B3d, B3e) with changed material properties for each beam. The length, height, and depth for all beams are kept constant and are taken as 1200 mm, 200 mm and 100 mm, respectively. Two different materials (Material 1 and Material 2) are used and changed at the point where the bending moment becomes zero, as shown in Figure 8. Young's modulus of material 1 is kept constant, and Young's modulus of material 2 is gradually changed for beam B3a, B3b, B3c, B3d, B3e. The criteria of serviceability have been ignored for this example because we here want to investigate the maximum change in shape with changing material for a predefined target maximum shear stress. The number of iterations and the system time taken by GSO and Optistruct to get the optimized shape of B3a, B3b, B3c, B3d, B3e, along with the percentage weight reduction, are shown in Table 4. The change in coordinates for the attainment of the final optimized shape obtained under the varying material property is indicated in Table 5.

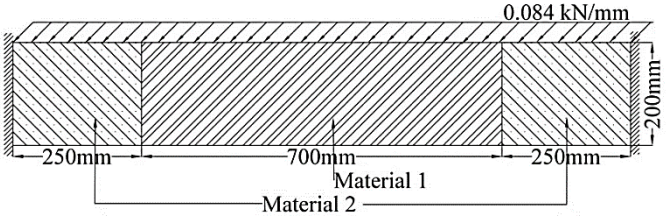

Figure 8. Schematic representation of beam B3.

Table 4. Parameters for B3a, B3b, B3c, B3d and B3e with iterations, runtime and percentage weight reduction to reach the optimized shape.

Type of B3 beams	σ_t (N/mm^2)	Iterations (Nos.)		Runtime (Sec.)		Weight Reduction (%)	
		GSO	Optistruct	GSO	Optistruct	GSO	Optistruct
B3a	50	35	6	08	24	75.32	62.01
B3b	50	43	4	17	28	75.40	63.53
B3c	50	106	5	38	20	78.08	66.71
B3d	50	159	6	40	24	78.11	66.40
B3e	50	79	4	28	17	79.32	63.54

Table 5. Final optimized shape of B3a, B3b, B3c, B3d and B3e.

Type of B3 beams	Material description (Young's Modulus)	GSO	Optistruct
B3a	Material 1 : 2.1x10^5 N/mm^2 Material 2: 0.2x10^5 N/mm^2	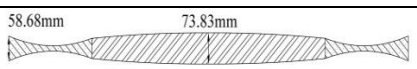	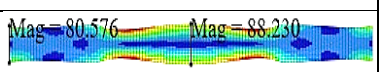
B3b	Material 1 : 2.1x10^5 N/mm^2 Material 2: 0.5x10^5 N/mm^2	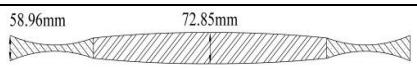	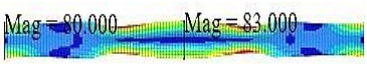
B3c	Material 1 : 2.1x10^5 N/mm^2 Material 2: 1.0x10^5 N/mm^2	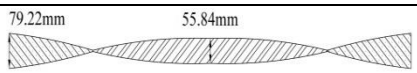	
B3d	Material 1 : 2.1x10^5 N/mm^2 Material 2: 1.5x10^5 N/mm^2	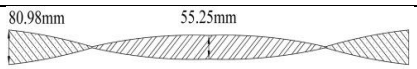	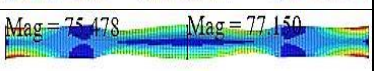
B3e	Material 1 : 2.1x10^5 N/mm^2 Material 2: 2.0x10^5 N/mm^2	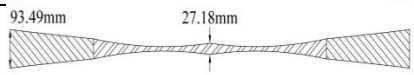	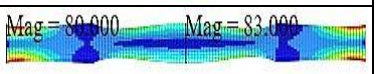

From the data obtained through validation and mesh convergence study in section 2, we can observe that GSO converges at an average element size of 50, which is much bigger than what is required by Optistruct, which converges at an average element size of 10. Hence, it can be inferred here that the suggested non-gradient method (GSO) requires much lesser dense mesh and far less computation to reach accuracy than what is required by the gradient descent method (Optistruct).

From the results obtained and illustrated in Table 1, Table 2 and Table 3, we can mark that the number of iterations needed by GSO to make it to the optimized shape is much more than that needed by Optistruct, but the time required per iteration in GSO is very much lesser than that required by Optistruct. The overall average time per iteration as obtained in the present study for GSO is 0.23 seconds, whereas, for Optistruct, it is 3.64 seconds. The reduction in weight under the given target maximum shear stress is comparable in both approaches. In structure B2 and CC, Optistruct has shown better weight reduction than GSO, whereas, in B1 and B3, GSO gives better results. However, the biggest difference comes in the final optimized shape obtained. In Optistruct, the final optimized shape shows more sharp corners than that obtained by GSO, causing more points of stress concentration as seen in B1, B2, B3 and CC. The shapes obtained under GSO have a smoother transition and shows more symmetricity even in asymmetrical loading as seen in B2 than that obtained under Optistruct. This makes the GSO method more fabricable and industry-friendly than Optistruct.

From the results obtained in Table 4 and Table 5, we can see that GSO is more responsive to the change in material property than Optistruct. The final shape obtained in Optistruct is almost the same with changing material properties, whereas the final shape obtained under GSO have changed significantly. As Young's modulus is increased from 0.2×10^5 N/mm^2 to 2.0×10^5 N/mm^2, the weight reduction for the same given target maximum shear stress of 50 N/mm^2 in each case has gradually increased from 75.32% to 79.32% in GSO. On the other hand, in Optistruct, there is no clear pattern of change in weight reduction with changing material properties.

4. Conclusion

Present work successfully discusses the structural shape optimizing capabilities of the suggested fuzzy-based integrated zero-order method comparing it with Optistruct, which is one of the most used industrial software for shape optimization. The entire technique is embodied in software coined GSO encapsulated as a FORTRAN code. The approach successfully interacts with the given constraints and changes in structure, maintaining the serviceability criteria. The most important task in GSO is to define correct design elements and selection of proper design nodes in order to achieve desired optimized shape with faster convergence without compromising the quality of results. The program's runtime is relatively short and doesn't necessitate higher processing and computational power from a computer. The final optimized shapes obtained by GSO shows fewer stress concentration areas and sharp corners and are more practical and adaptable by industry than those obtained by Optistruct. Further future works on reducing the number of iteration to get the final optimized shape using neural networks are being looked after.

Conflict of Interest

The authors confirm that there is no conflict of interest to declare for this publication.

Acknowledgements
This research did not receive any specific grant from funding agencies in the public, commercial, or not-for-profit sectors. The authors would like to thank the editor and anonymous reviewers for their comments that helped improve the quality of this work.

References

Altair Engineering Inc. Optistruct (2019). 1 help _les, 2019.

Balamurugan, R., Ramakrishnan, C., & Singh, N. (2008). Performance evaluation of a two stage adaptive genetic algorithm (tsaga) in structural topology optimization. *Applied Soft Computing, 8*, 1607–1624.

Balamurugan, R., Ramakrishnan, C., & Swaminathan, N. (2011). A two phase approach based skeleton convergence and geometric variables for topology optimization using genetic algorithms. *Structural and Multidisciplinary Optimization*, *43*(3), 381–404.

Baumgartner, A., Harzheim, L., & Mattheck, C. (1992). SKO (soft kill option): The biological way to find an optimum structure topology. *International Journal of Fatigue, 14,* 387–393.

Bennett, J. A., & Botkin, M. E. (1985). Structural shape optimization with geometric description and adaptive mesh refinement. *American Institute of Aeronautics and Astronautics Journal 23*, 458-464.

Berke, L., Patnaik, S. N., & Murthy, P. L. N. (1992). Optimum design of aerospace structural components using neural networks. *Computers & Structures*, *48*(6), 1001–1010.

Chaube, S., & Singh, S. B. (2016). Fuzzy reliability theory based on membership function. *International Journal of Mathematical, Engineering and Management Sciences, 1*(1), 34–40.

Chen, J. L., & Tsai, W. C. (1993). Shape optimisation by using simulated biological growth approaches. *American Institute of Aeronautics and Astronautics Journal, 31*, 2143-2147.

Cuevas, E., Gálvez, J., & Avalos, O. (2020). Studies in computational intelligence. *Recent Metaheuristics Algorithms for Parameter Identification.*

Dong, Y., Yao, X., & Xu, X. (2020). Cross-section shape optimization design of fabric rubber seal. *Composite Structures, 256*, 113047.

Georgiou, G., Vio, G. A., & Cooper, J. E. (2014). Aeroelastic tailoring and scaling using bacterial foraging optimisation. *Structural and Multidisciplinary Optimisation, 50*(1), 81–99.

Guest, J. K., & Genut, L. C .S. (2010). Reducing dimensionality in topology optimization using adaptive design variable fields. *International Journal of Numerical Methods in Engineering, 81*, 1019–1045.

Hasengawa, A. (1992). Shape optimization of two dimensional bodies by boundary changing method and thickness changing method. *International Journal of Numerical Methods in Engineering, 34,* 889–892.

IS 456:2000. Plain and reinforced concrete—Code of practice.

Jarraya, A., Dammak, F., Abid, S., & Haddar, M. (2007). Shape and thickness optimization performance of a beam structure by sequential quadratic programming method. *Journal of Failure Analysis and Prevention, 7*(50), 50–55.

Kaveh, A., Hassani, B., Shojaee, S., & Tavakkoli, S. M. (2008). Structural topology optimization using ant colony methodology. *Engineering Structures, 30,* 2559–2565.

Kosheleva, O., Kreinovich, V., & Shahbazova, S. (2018, May). Type-2 fuzzy analysis explains ubiquity of triangular and trapezoid membership functions. In 2018 *Proceedings of the 7th World Conference on Soft Computing* (pp. 1–6). Baku, Azerbaijan.

Krishnamoorthy, C. S. (1994). *Finite element analysis theory and programming*. Delhi: New McGraw Hill.

Kumar, A., Bisht, S., Goyal, N., & Ram, M. (2021). Fuzzy reliability based on hesitant and dual hesitant fuzzy set evaluation. *International Journal of Mathematical, Engineering and Management Sciences*, *6*(1), 166–179.

Lee, K., & Geem, Z. (2004). A new structural optimization method based on the harmony search algorithm. *Computer and Structures*, *82*, 781–798.

Luh, G. C., Lin, C. Y., & Lin, Y. S. (2011). A binary particle swarm optimization for continuum structural topology optimization. *Applied Soft Computing*, *11*, 2833–2844.

Luh, G., & Chueh, C. (2004). Multi-model topological optimization of structure using immune algorithm. *Computer Methods in Applied Mechanics and Engineering*, *193*, 4035–4055.

Manan, A., Vio, G. A., Harmin, M. Y., & Cooper, J. E. (2010). Optimisation of aeroelastic composite structures using evolutionary algorithms. *Engineering Optimization*, *42*, 171–184.

Mattheck, C. (1989). Biological shape optimisation of mechanical components based on growth. In *Proceedings on the International Congress on Finite Element Method* (pp. 167–176).

Mattheck, C., & Burkhardt, S. (1990). A new method of structural shape optimisation based on biological growth. *International Journal of Fatigue*, *12*, 185–190.

Mei, L., & Wang, Q. (2021). Structural optimization in civil engineering: A literature review. *Buildings*, *11*(2), 1–28.

Mohandas, S. U., Phelp, T. A., & Ragsdell, K. M. (1990). Structural optimization using a fuzzy goal programming approach. *Computers and Structures*, *37*(1), 1–8.

Mortazavi, A. (2020). A new fuzzy strategy for size and topology optimization of truss structures. *Applied Soft Computing Journal*, *93*, 106412.

Mortazavi, A. (2020). Large-scale structural optimization using a fuzzy reinforced swarm intelligence algorithm. *Advances in Engineering Software*, *142*, 102790.

Munk, D. J., Vio, G. A., & Steven, G. P. (2015). Topology and shape optimization methods using evolutionary algorithms: A review. *Structural and Multidisciplinary Optimization*, *52*(3), 613–631.

Nagy, A. P., Abdalla, M. M., & Gürdal, Z. (2009). Isogeometric sizing and shape optimization of beam structures. *Computer Methods in Applied Mechanics and Engineering*, *199*, 1216–1230.

Pathak, K. K., Sehgal, D. K., Akhtar, S., & Bhadauria, S. S. (2007). A review of structural shape ptimization techniques. *Journal of Structural Engineering*, *33*(6), 505–514.

Rispler, A. R., Tong, L., Steven, G. P., & Wisnom, M. R. (2000). Shape optimisation of adhesive fillets. *International Journal of Adhesion and Adhesives*, *20*, 221–231.

Shim, P. Y., & Manoochehri, S. (1997). Generating optimal configurations in structural design using simulated annealing. *International Journal of Numerical Methods in Engineering*, *40*, 1053–1069.

Soh, C. K., & Yang, J. (1996). Fuzzy controlled genetic algorithm search for shape optimization. *Journal of Computing in Civil Engineering*, *10*(2), 143–150.

Upadhyay, B. D., Sonigra, S. S., & Daxini, S. D. (2021). Numerical analysis perspective in structural shape optimization: A review post 2000. *Advances in Engineering Software*, *155*, 102992.

Wang, S., & Tai, K. (2005). Structural topology design optimization using genetic algorithms with a bit-array representation. *Computer Methods in Applied Mechanics and Engineering*, *194*, 3749–3770.

Wu, Z. (2005). An efficient approach for shape optimization of components. *International Journal of Mechanical Sciences*, *47*, 1595–1610.

Zienkiewicz, O. C., & Taylor, R. L. (1991). *The finite element method* (Vol. 1 & 2, 4th ed.). London: McGraw Hill.

Zimmermann, H. J. (1996). *Fuzzy set theory*. Dordrecht: Kluwer.